Green Chemistry

View Online
Dynamic Article Links

Cite this: *Green Chem.*, 2011, **13**, 1517

www.rsc.org/greenchem

PAPER

Separation of ethanol–water mixtures by liquid–liquid extraction using phosphonium-based ionic liquids†

Catarina M. S. S. Neves,[a] José F. O. Granjo,[b] Mara G. Freire,[a] Al Robertson,[c] Nuno M. C. Oliveira[b] and João A. P. Coutinho*[a]

Received 20th January 2011, Accepted 28th March 2011
DOI: 10.1039/c1gc15079k

Bio-alcohols are produced from biomass by fermentation, and distillation is commonly used to separate the alcohol from the aqueous phase. This is, however, a high energy consumption process, and alternative approaches to this separation are being pursued. In this work, the use of phosphonium-based ionic liquids (ILs) for the extraction of ethanol from fermentation broths is investigated. Ternary phase diagrams, necessary for the design and to implement an alternative liquid–liquid extraction process for the alcohol recovery, were determined for seven ionic liquids. The modelling of the equilibrium data was performed using the COSMO-RS and NRTL models; the first aiming at screening other ionic liquids not experimentally studied, and the latter aiming at designing a separation process. The gathered data indicate that phosphonium-based ionic liquids are the best yet reported to perform water–ethanol separations. Based on the most promising phase diagrams, an analysis of the alcohol and ionic liquid recovery steps was carried out and a liquid–liquid extraction stage coupled to an extractive fermentation, where the ionic liquid is continuously recycled to the fermentator and the ethanol concentration is carried out by pervaporation, is here proposed as an alternative to distillation.

Introduction

The continuous depletion of oil reservoirs, the increasing oil extraction costs, the emergence of new economies where oil demand is rising exponentially, and the unstable political situation coupled to the occurrence of natural disasters in oil producing areas, are forcing governments to redefine their energetic strategies to maintain a sustainable social development. Significant environmental concerns result from an incessant consumption of petroleum-based fuels. The combustion of fossil fuels leads to emissions of greenhouse gases and other pollutants, such as NO_x, SO_x, CO and organic volatile compounds. Consequently, a strong effort is currently being directed towards the development of sustainable alternatives to fossil fuels.

Bioethanol is being actively studied as an alternative for transportation fuels, used either as an additive to gasoline or as a stand-alone fuel. It can be produced from a variety of renewable staples and, hopefully, in the near future from a variety of lignocellulosic raw materials – that are widely available and do not compete with the production of food crops. It allows a cleaner combustion, reducing the emission of hazardous gases to the atmosphere, and may have an important contribution to reduce CO_2 emissions and fossil fuels dependency.[1]

Bioethanol is produced by the fermentation of carbohydrates. One of the main issues associated with its production is the purification from fermentation broths. If ethanol is produced from pentoses, alcohol concentrations are usually below 5 wt% .[2] Though in general this separation is technically not very challenging for ethanol concentrations in the 5–15% range,[2] since it can be achieved through common distillation, it nevertheless entails high energy consumption. According to Vane,[3] the energy required to separate ethanol from water by distillation typically amounts to 10% of the energetic content of the recovered ethanol. This value increases exponentially for ethanol concentrations below 10 wt%. For instance, with an ethanol solution of 6 wt% that energy cost corresponds to 17%, while for a 2 wt% alcohol mixture this value reaches 50% of the energetic content of ethanol in the mixture.[3] Hence, a significant amount of energy is expended in the first concentration step, the so called beer column, for the purification

[a]*Departamento de Química, CICECO, Universidade de Aveiro, 3810-193, Aveiro, Portugal. E-mail: jcoutinho@ua.pt; Fax: +351-234-370084; Tel: +351-234-370200*
[b]*CIEPQPF, Departamento de Engenharia Química, Universidade de Coimbra, 3030-790, Coimbra, Portugal*
[c]*Cytec Canada Inc., 9061 Garner Road, Niagara Falls, Ontario, Canada L2E 6S5*

† Electronic supplementary information (ESI) available: Experimental weight fraction data for the systems IL + water + EtOH, *S* and *D* dependence on the ethanol content, and NRTL parameters estimation. See DOI: 10.1039/c1gc15079k

of ethanol through a typical distillation. On the other hand, at the opposite concentration extreme, distillation is only effective up to approximately 85 wt% of ethanol. Above this turnover composition, the recovery of ethanol becomes more difficult to accomplish (due to the decrease in the volatility towards the azeotropic point), requiring the use of complementary approaches to attain anhydrous ethanol.[2,3]

In addition to the above limitations, when the manufacture of ethanol from lignocellulosic sources is considered, important differences in the production scales can be dictated by the availability of the raw materials, and new opportunities for energy and mass integration appear in the context of the additional processing steps that compose a typical biorefinery. These new features can make the classical solutions for ethanol purification less attractive in this novel context, thus requiring a systematic evaluation of alternative separation technologies.[2,4]

Arlt and co-workers[5,6] were the first to propose the use of ionic liquids (ILs) as potential solvents in extractive distillation to separate water–ethanol mixtures. The authors studied imidazolium-based ILs, with chloride and tetrafluoborate anions, and concluded that these ionic solvents are improved entrainers, capable of breaking the water–ethanol azeotrope.[6] Thereafter, a number of academic studies followed this work questing for ILs able to effectively break the azeotropic mixture.[7–10]

Another approach, less energy intensive, used for the separation of ethanol–water mixtures is liquid–liquid extraction, especially when coupled with the use of extractive fermentations.[2,3] Boudreau and Hill[11] reported that liquid–liquid extraction could reduce the energy consumption on the ethanol–water separation by *circa* 40% when compared with the distillation technique. Fadeev and Meagher[12] reported the pioneer work on the use of ILs for the separation of alcohol-water mixtures by liquid–liquid extraction. The authors suggested the use of hexafluorophosphate-based ILs. In addition, Swatloski *et al.*[13] presented ternary phase diagrams for ethanol + water + IL systems, while Najdanovic–Visak *et al.*[14,15] further explored these systems through the evaluation of the alcohol effect in the water-IL phase behaviour. Yet, both $[BF_4]^-$ and $[PF_6]^-$ anions are not water stable under particular conditions,[16] and further studies with ILs based on water stable anions were later reported by Najdanovic–Visak *et al.*[17] However, the type 3 phase diagrams obtained, with all the pairs of compounds exhibiting only partial miscibility, are not favourable for a selective extraction of ethanol from aqueous-rich phases. Recently, Chapeaux *et al.*[18] reported the ternary phase diagrams for 1-hexyl-3-methylimidazolium bis(trifluoromethylsulfonyl)imide (the IUPAC standard IL), water and two alcohols: ethanol and 1-butanol. The authors concluded that although both systems could be used for the separation of alcohol-water mixtures, the ethanol selective separation was not very favourable.

Most studies comprising ILs have been focused in imidazolium-based compounds. Phosphonium-based ILs, despite their advantages (less expensive and thermally more stable than the equivalent imidazolium-based counterparts, availability on a multi-ton scale,[19] and have already been used in industrial processes[20]) have received little attention. As a result of their advantages, phosphonium-based ILs are particularly interesting candidates for liquid–liquid extraction purposes. Moreover, unlike most ILs, they are less dense than water, facilitating the use of conventional units designed for systems that require the aqueous phase decantation. Regarding the few works considering phosphonium-based ILs, Domańska and co-workers[21–24] have been studying their phase equilibria with alcohols and hydrocarbons. In our lab we have studied their thermophysical properties,[25,26] their phase equilibria with water,[26,27] have shown that they are better than imidazolium-based ILs at dissolving carbon dioxide,[28–30] their potential use in the extraction of diamondoids from natural gas[31] and their application in aqueous two phase systems aiming at purifying value-added biomolecules.[32] Still, from the best of our knowledge, phosphonium-based ILs have not been previously studied for the selective separation of ethanol–water mixtures.

Aiming at developing efficient liquid–liquid extraction techniques for the selective separation of ethanol–water mixtures, a large range of phosphonium-based ILs were investigated here. This study was carried out using tetradecyltrihexylphosphonium-based ILs ($[TDTHP]^+$) combined with different anions: *viz.* dicyanamide ($[N(CN)_2]^-$); bromide (Br^-); chloride (Cl^-); bis(trifluoromethylsulfonyl)imide ($[NTf_2]^-$); bis(2,4,4-trimethylpentyl)phosphinate ($[Phosph]^-$); decanoate ($[Deca]^-$) and methanesulfonate ($[CH_3SO_3]^-$). Experimental measurements of liquid–liquid equilibrium (LLE) tie-lines for ternary systems (water + ethanol + IL) were carried out for each of the described ILs at 298 K. Moreover, the resulting experimental data were modelled using the NRTL free energy model. A good agreement with the experimental data was obtained, allowing a straightforward description of these ternary systems for process design calculations. The experimental results were also compared with predictions obtained from the COSMO-RS application. Due to its fundamental nature, and although not always providing satisfactory results on the compositions of the two co-exisiting phases, this model was able to predict the phase behavior of the systems studied and the ILs trend, without the need of using experimental LLE data in advance. Due to its predictive capability, the COSMO-RS model was also used to evaluate the LLE of additional [TDTHP]-based ILs with different anions (for which experimental data are currently not available), aiming at screening tailored ILs with improved features towards the extraction of ethanol.

Experimental results

The chemical structures of the phosphonium-based ILs studied in this work are depicted in Fig. 1. The tie-lines measured for the seven ternary systems considered are displayed in the ternary phase diagrams presented in Fig. 2 to 8, along with the modelling results obtained both by COSMO-RS and NRTL. The phase equilibrium compositions, and a simultaneous comparison between all the experimental results obtained, are presented in the ESI.† The consistency of the tie-lines was checked using the Othemer-Tobias correlation,[33] and the correlation for each system is also provided in the ESI.†

All the phosphonium-based ILs investigated are fully soluble in ethanol while presenting limited solubility in water (below 10^{-5} in a mole fraction basis). The water solubility in ionic liquids is more significant and ranges from 2.2 wt% for $[TDTHP][NTf_2]$ to 16 wt% for [TDTHP][Phosph]. The water solubility increase

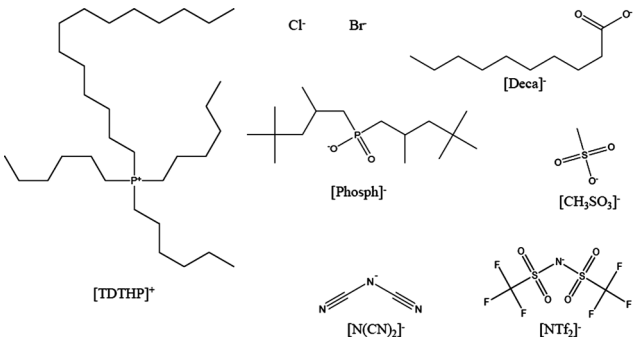

Fig. 1 Chemical structures of the common IL cation ([TDTHP]$^+$) combined with the different anions studied in this work.

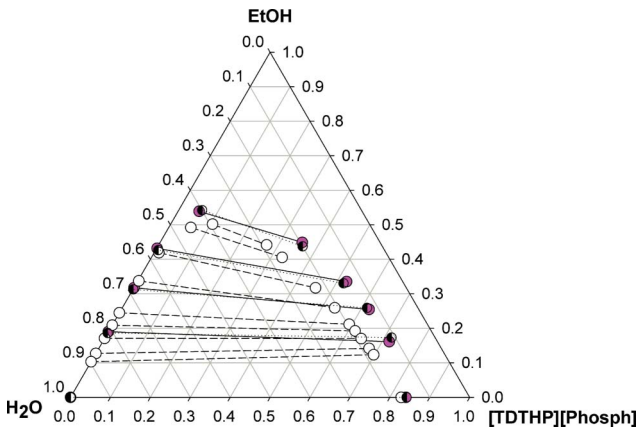

Fig. 2 Ternary phase diagram for the system [TDTHP][Phosph] + EtOH + H_2O at 298 K (mass fraction units). The full symbols and the solid lines represent the experimental data, the semi-filled symbols and the dotted lines represent the correlation by the NRTL model, and the empty symbols and the dashed lines represent the prediction by COSMO-RS.

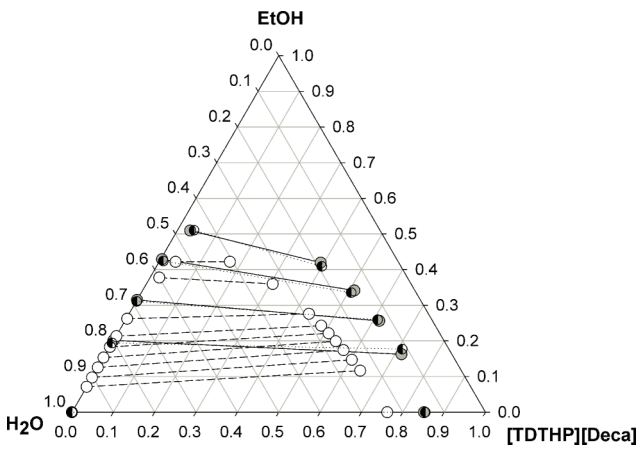

Fig. 3 Ternary phase diagram for the system [TDTHP][Deca] + EtOH + H_2O at 298 K (mass fraction units). The full symbols and the solid lines represent the experimental data, the semi-filled symbols and the dotted lines represent the correlation by the NRTL model, and the empty symbols and the dashed lines represent the prediction by COSMO-RS.

in ILs follows the anion trend $[NTf_2]^- < [N(CN)_2]^- < Br^- < Cl^- \approx [CH_3SO_3]^- < [Deca]^- < [Phosph]^-$. The water solubility results obtained are in good agreement with those previously

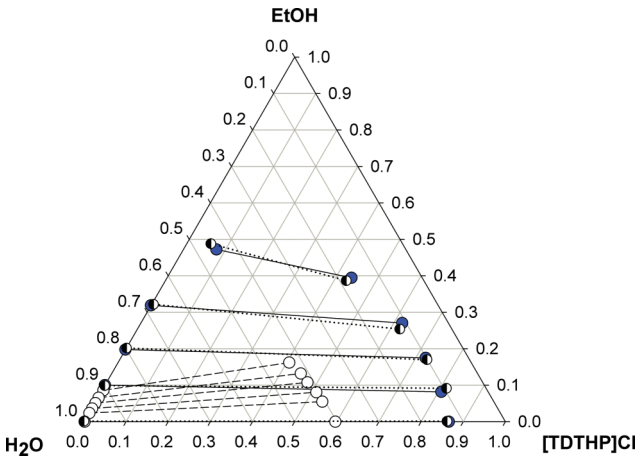

Fig. 4 Ternary phase diagram for the system [TDTHP]Cl + EtOH + H2O at 298 K (mass fraction units). The full symbols and the solid lines represent the experimental data, the semi-filled symbols and the dotted lines represent the correlation by the NRTL model, and the empty symbols and the dashed lines represent the prediction by COSMO-RS.

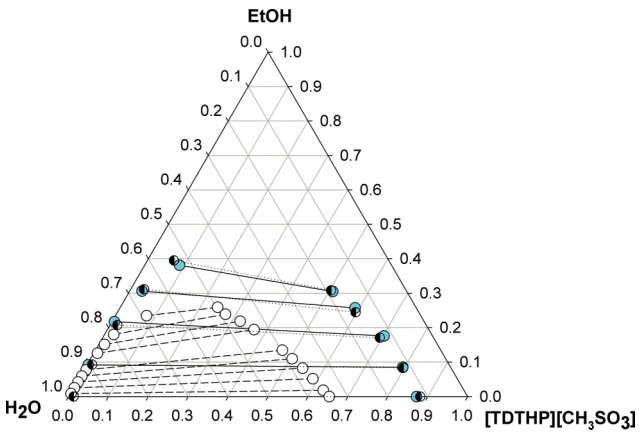

Fig. 5 Ternary phase diagram for the system [TDTHP][CH_3SO_3] + EtOH + H_2O at 298 K (mass fraction units). The full symbols and the solid lines represent the experimental data, the semi-filled symbols and the dotted lines represent the correlation by the NRTL model, and the empty symbols and the dashed lines represent the prediction by COSMO-RS.

reported.[26,27] The critical points for each system, estimated by applying the Sherwood method,[34] are reported in the ESI.†

All of the ternary systems studied exhibit type 1 liquid–liquid phase diagrams, where partial miscibility is only observed in the IL-water binary system, presenting thus large biphasic regions. The two phase region envelope decreases with the water solubility trend presented above. In fact, the [NTf_2]-based system presents the largest two phase region observed in this work. As a result, the water solubility values in all ILs (binary systems results) can be used as an initial guide to identify promising ILs for ethanol extraction. This criterion is important since due to the non-volatile nature of ILs, it is possible to obtain ethanol-rich phases by liquid–liquid extraction, followed by evaporation of the volatile components in the extract and recycle of the IL. Using this approach, ILs with a larger two phase region lead to higher ethanol concentrations after a proper evaporation step, and are therefore preferable from a selectivity viewpoint.

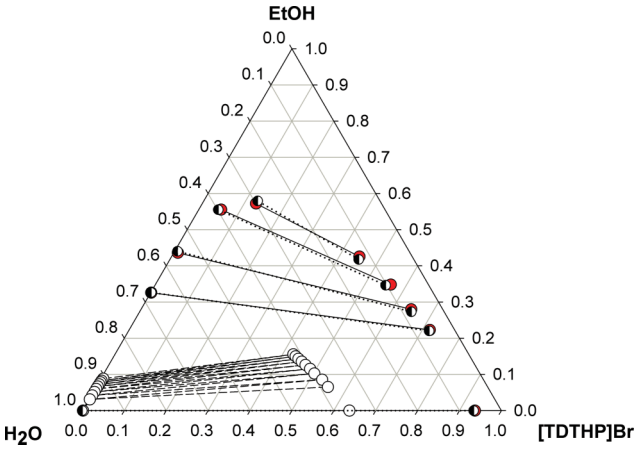

Fig. 6 Ternary phase diagram for the system [TDTHP]Br + EtOH + H_2O at 298 K (mass fraction units). The full symbols and the solid lines represent the experimental data, the semi-filled symbols and the dotted lines represent the correlation by the NRTL model, and the empty symbols and the dashed lines represent the prediction by COSMO-RS.

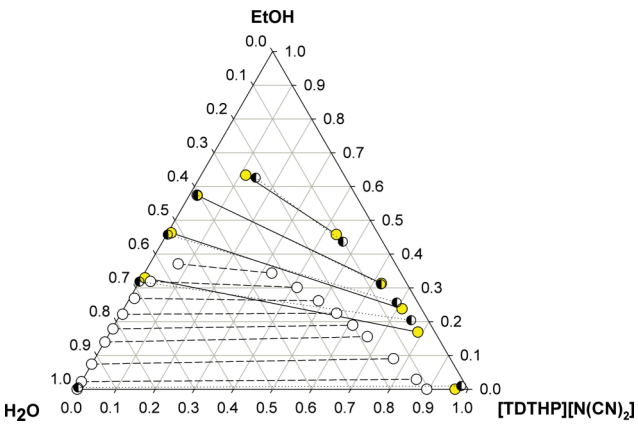

Fig. 7 Ternary phase diagram for the system [TDTHP][$N(CN)_2$] + EtOH + H_2O at 298 K (mass fraction units). The full symbols and the solid lines represent the experimental data, the semi-filled symbols and the dotted lines represent the correlation by the NRTL model, and the empty symbols and the dashed lines represent the prediction by COSMO-RS.

The two phase regions of phosphonium-based systems are in general larger than those previously observed for imidazolium-based ionic liquids with the same anion.[18] The maximum ethanol concentration that can be reached by each system was estimated from the ternary phase diagrams by identifying the point in the IL-rich phase that by removal of the IL would produce a mixture with the highest concentration in ethanol. These ethanol concentrations are reported in Table 1. The ethanol concentrations range from 65 wt% with [TDTHP][CH_3SO_3] to *circa* 90 wt% using [TDTHP][NTf_2]. These values compare with a maximum reported by Chapeaux *et al.*[18] of approximately 65 wt% with [HMIM][NTf_2] (1-hexyl-3-methylimidazolium bis(trifluoromethylsulfonyl)imide). As a result, phosphonium-based ILs combined with appropriate anions can be viewed as potential improved candidates for the extraction of ethanol from fermentation broths. Additional characteristics of phosphonium-based ILs, such as lower toxicity compared to imidazolium-based media, are also discussed below.

Table 1 Ethanol distribution coefficients and selectivities for each system at the composition of 20 wt% of ethanol, calculated by the correlation of *D* and *S* along with the ethanol content, and the maximum ethanol concentration obtainable by complete evaporation from the IL-rich phase (all values reported in mass basis)

System	*D*	*S*	Maximum EtOH extraction (%)
[TDTHP][Phosph]	0.83	5.1	72
[TDTHP][Deca]	0.82	4.9	70
[TDTHP]Cl	0.88	6.6	72
[TDTHP][CH_3SO_3]	0.82	4.6	65
[TDTHP]Br	0.70	8.4	78
[TDTHP][$N(CN)_2$]	0.51	6.8	82
[TDTHP][NTf_2]	0.31	2.0	87
[TDTHP][$B(CN)_4$]	—	—	91[a]
[TDTHP][$C(CN)_3$]	—	—	80[a]

[a] Predicted by COSMO-RS.

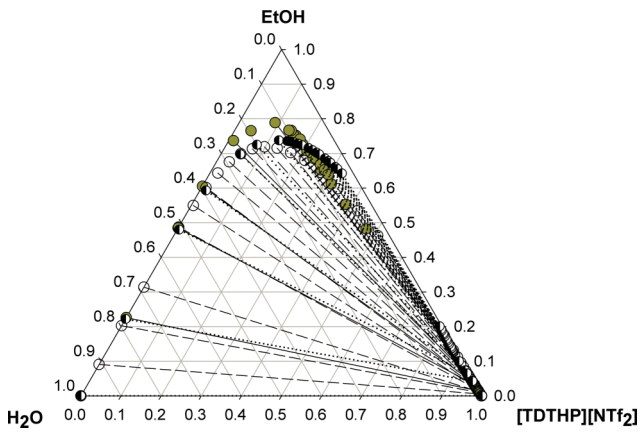

Fig. 8 Ternary phase diagram for the system [TDTHP][NTf_2] + EtOH + H_2O at 298 K (mass fraction units). The full symbols and the solid lines represent the experimental data, the semi-filled symbols and the dotted lines represent the correlation by the NRTL model, and the empty symbols and the dashed lines represent the prediction by COSMO-RS.

Table 1 also presents the ethanol distribution coefficients (*D*) and selectivities (*S*) between the two phases: IL-rich phase (IL) and aqueous-rich phase (aq). The distribution coefficients are defined as

$$D = w_{\mathrm{EtOH}}^{\mathrm{IL}} / w_{\mathrm{EtOH}}^{\mathrm{aq}} \quad (1)$$

where w_{EtOH} represents the mass fraction of ethanol at each phase, while *D* expresses the relative capacity of the IL to remove ethanol from aqueous mixtures. The selectivity of each system for ethanol was determined using eqn (2)

$$S = \frac{w_{\mathrm{EtOH}}^{\mathrm{IL}} / w_{\mathrm{W}}^{\mathrm{IL}}}{w_{\mathrm{EtOH}}^{\mathrm{aq}} / w_{\mathrm{W}}^{\mathrm{aq}}} \quad (2)$$

where the subscripts *EtOH* and *W* designate ethanol and water, respectively. *S* indicates the ability of each IL to selectively remove ethanol.

The determined ethanol distribution coefficients and selectivities can be used to compare the performances of the current ILs with alternative solvents previously studied for the ethanol recovery through liquid–liquid extraction.[11–15,17,18,35] In Table 1 for a 20 wt% of ethanol composition, the distribution coefficients range from 0.3 to 0.9, while the ethanol selectivities vary between 2 and 8. These values correspond to reasonable values in the range of known alternative solvents, given that D is reported in a mass fraction basis. The exception to this pattern appears to be the [NTf_2]-based IL, that presents both low selectivities and distribution coefficients for a 20 wt% of ethanol solution. Nevertheless, it should be reminded that this IL displays improved selectivity for low concentrations of ethanol (see ESI†). For comparison, under approximately similar conditions the [HMIM][NTf_2] system studied by Chapeaux *et al.*[18] presented values of $D = 0.15$ and $S = 11$, which translate into better selectivity but a lower solvent capacity for ethanol. Considering the maximum ethanol concentrations reported in Table 1, while for the systems studied, liquid–liquid extraction cannot be directly used to break the ethanol–water azeotrope, the possibility of using this approach in concentrating ethanol from dilute aqueous solutions will be analysed below, in the context of reducing the energy costs required in the ethanol purification process.

COSMO-RS model predictions

The COSMO-RS model (COnductor-like Screening MOdel for Real Solvents) allows the prediction of the fluids phase equilibria using unimolecular quantum calculations coupled to statistical thermodynamic approaches.[36–40] Previous studies applied COSMO-RS for predicting the LLE of binary systems of ILs and the most diverse molecular solvents, namely alcohols, hydrocarbons, ethers, ketones and water.[27,41–49] Nevertheless, few publications have considered the application of COSMO-RS (or related modified versions) to ternary systems containing ILs.[50–52] Gibbs free energy models such as non-random two liquids (NRTL), or universal quasi-chemical (UNIQUAC), group-contribution methods (GCMs) and equations of state (EoS) require experimental data to estimate the model intrinsic parameters. Alternatively, COSMO-RS is a purely predictive model, and therefore can be highly valuable in the investigation of systems involving ILs where experimental data are not yet available. Considering the large number of possible ILs, including their combination with molecular solvents, the availability of predictive methods appears to be extremely convenient since they can be used as screening tools to select ILs for specific applications.

The ternary phase diagrams measured were used to evaluate the performance of the COSMO-RS model in the prediction of the LLE of these systems. In agreement with results previously reported[27] with the bromide and chloride anions, COSMO-RS is unable to provide enhanced quantitative descriptions of the phase diagrams. However, for the remaining systems, a reasonable prediction of the binodal curves is achieved, as shown in Fig. 2, 3, 7 and 8, where the predicted phase diagrams for the ILs with phosphinate, decanoate, $[N(CN)_2]^-$ and $[NTf_2]^-$ are compared with the experimental data. Nevertheless, it should be pointed out that in most systems the predictions by COSMO-RS for the compositions of each component at both co-existing phases is still far from the experimental data. As previously observed,[45,46,53,54] COSMO-RS can provide a good description of the LLE data when the compounds are poorly miscible. Since the COSMO-RS calculations consider that the interactions are made on the conductor interface surrounding the molecules (thus treated as isolated species), stronger interactions responsible for larger mutual solubilities are not adequately taken into account by COSMO-RS. Given the large biphasic regions presented by these systems, and on the qualitative trends predicted by COSMO-RS, it seems that COSMO-RS can be used to investigate the suitability of other non fluorinated anions for the ethanol–water separation. While much less precise than the experimental measurements on providing the phase diagrams, COSMO-RS allows the screening of ILs not currently available, which can be further synthesized and used in experimental approaches.

The COSMO-RS was used to study the ternary phase diagrams of a series of [TDTHP]-based ILs combined with different anions, such as methylsulfate ($[CH_3SO_4]^-$), ethylsulfate ($[C_2H_5SO_4]^-$), tosylate ($[Tos]^-$), tetracyanoborate ($[B(CN)_4]^-$) and tricyanomethane ($[C(CN)_3]^-$). While the predicted ternary phase diagrams for most of these ILs were not satisfactory with respect to the objective of this work, systems with tetracyanoborate ($[B(CN)_4]^-$) and tricyanomethane ($[C(CN)_3]^-$) seem promising in the selective extraction of ethanol, and further experimental measurements on these systems are immediately envisaged. Fig. 9 presents the predicted ternary phase diagrams for the [TDTHP][$B(CN)_4$] and [TDTHP][$C(CN)_3$] ILs. Table 1 also lists the estimated maximum ethanol concentrations that can be obtained by complete evaporation of the extract phases resulting from these systems. Thus, although not yet experimentally available, the cyano-based ILs appear as potential solvents regarding the ethanol extraction from aqueous phases.

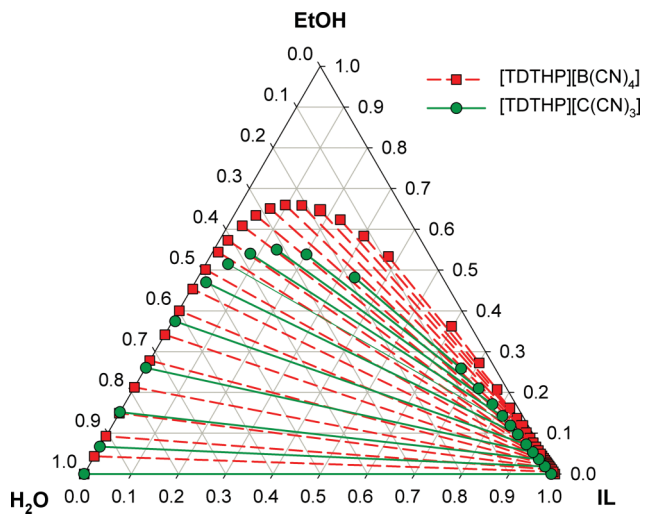

Fig. 9 Prediction of the ternary phase diagrams for the systems [TDTHP][$B(CN)_4$] + EtOH + H_2O and [TDTHP][$C(CN)_3$] + EtOH + H_2O at 298 K (mass fraction units) by COSMO-RS.

Modeling the LLE data with NRTL

The NRTL model[55] has been successfully used over a wide range of vapour-liquid equilibrium (VLE) and LLE systems

Table 2 NRTL binary interaction parameters and average absolute deviations between the experimental mass fraction compositions and NRTL correlation results, for each system at 298 K

Ionic liquid	NRTL binary interaction parameters				Average absolute deviation ($\lvert w_{exp}-w_{NRTL} \rvert$)		
	τ_{13}	τ_{31}	τ_{23}	τ_{32}	w_{IL}	w_{EtOH}	w_{H_2O}
[TDTHP][Phosph]	25.25	−1.450	6.064	−3.917	0.004	0.006	0.005
[TDTHP][Deca]	23.82	−1.169	5.487	−3.559	0.005	0.006	0.005
[TDTHP]Cl	11.14	−2.555	5.230	−3.181	0.006	0.007	0.008
[TDTHP][CH_3SO_3]	11.09	−3. 487	5.998	−3.318	0.009	0.006	0.006
[TDTHP]Br	21.09	6.265	4.688	−2.760	0.003	0.003	0.005
[TDTHP][$N(CN)_2$]	14.82	1.313	4.865	−2.873	0.016	0.012	0.010
[TDTHP][NTf_2]	11.36	4.674	4.798	−1.520	0.024	0.023	0.002

to describe the non-ideality in the liquid phase. It is based on the local composition concept to express the effect of the intermolecular forces (short-range) in the non-randomness of the mixtures. One of the main advantages of NRTL is that multicomponent LLE and VLE can be predicted using only binary interaction parameters, which can be estimated from experimental data. For each binary molecular pair *i*-*j*, the model has three parameters – two interaction parameters τ_{ij} and τ_{ji} and the non-randomness parameter α_{ij} ($\alpha_{ij} = \alpha_{ji}$). Parameters τ_{ij} are related to the Gibbs free energy of interaction between a specie *i* around a central specie *j* (Δg_{ij}) in a hypothetical cell in the liquid. The parameter α_{ij} is related to the lattice structure of the liquid and it is proportional to 2/Z, where Z is the lattice coordination number of the liquid (this varies commonly from 8 to 12; 10 is usually considered).

Although the NRTL model was not developed to describe the behaviour of solutions containing electrolyte species, it has found successful application in ternary water + alcohol + IL LLE systems.[18,56–59] This can be related to the fact that in ILs the ion charge is usually dispersed and the long-range electrostatic forces are weak compared with the short-range intermolecular forces (so that they can be neglected), and thus allowing the applicability of the NRTL model.

The use of the NRTL model to correlate the LLE data should be seen as a first choice of a simple theoretical model that could provide a reasonably precise description of the equilibrium conditions, while being of practical value for design calculations. This also provides a comparison of the accuracies obtained with simpler equilibrium models, used in data regression, and the predictions of more complex models, such as COSMO-RS.

Different approaches have been considered for the parameter estimation problem with the NRTL model to obtain the best set of parameters that describe the LLE data available.[58,60] In the present work, this task was formulated as the solution of a nonlinear programming problem, using the weighted norm of the differences between the experimental mass fractions and the values predicted by the model as the objective function, as described by eqn (3):[60]

$$\min_{z} \phi = \sum_{i}^{n_t} \sum_{j}^{n_c} \sum_{k}^{2} \omega_{ijk} e_{ijk}(\tau)^2 \qquad (3)$$

Here $e_{ijk}(\tau) = w^{exp}{}_{ijk} - w^{mood}{}_{ijk}(\tau)$, where the superscripts *exp* and *mod* correspond to the experimental and calculated mass fraction values, respectively. The summations in this equation are taken over all tie-lines (*i*), components (*j*) and phases (*k*), and ω_{ijk} is a weight factor associated with each error term. Using the isothermal data available for each system, the objective function ϕ was minimized by simultaneous determination of all unknowns (composition variables and model parameters, here collectively denoted by *z*), subject to constraints of isoactivity, the NRTL activity coefficient model, sum of mass and molar fraction restrictions, and magnitude bounds for the model parameters τ_{ij}. Mass fractions were used in the data regression, due to the large differences in molecular weights between the ILs and the molecular components. More details about the NRTL parameter estimation are presented in the ESI.†

Since the experimental data available were registered at only one temperature, the α_{ij} parameters in the model were considered constant, and equal to recommended values for each pair of components in the mixture. Values of $\alpha_{13} = 0.2$ and $\alpha_{23} = 0.3$ were used as suggested by Song and Chen.[61] The parameters τ_{12}, τ_{21} and α_{12}, referring to the water–ethanol binary pair, were retrieved from existing data by Song and Chen,[61] and are given by $\alpha_{12} = 0.3031$, $\tau_{12} = 670.4/T$ and $\tau_{21} = -55.2/T$. The weights ω_{ijk} were considered to be unitary for all data points available. Table 2 summarizes the values obtained for the optimized parameters of the NRTL model.

From the ternary phase diagrams displayed in Fig. 2 to 8, it is possible to observe that the NRTL model is able to provide a close fit to the experimental data. Results for the absolute deviation between the experimental data and correlated results, for each tie-line and each system, are presented in the ESI.† The average of absolute deviations between the experimental data and the NRTL correlated results are presented in Table 2. The main exception was observed with the [NTf_2]-based system, where the NRTL model shows more difficulties in providing an exact representation of the binodal curve, giving the localization of the critical point in the right branch at a relatively low concentration of ethanol. To achieve these results with the [NTf_2]-based system, additional experimental measurements of the composition of the water phase along the saturation line are required, since the values of the parameters displayed a high sensitivity to the data available in this region. The experimental saturation line was completed using the cloud point titration method, and the respective data points are also presented in Fig. 8.

The relative precision of the NRTL model description of the experimental data is comparable to the quality of the regressions for other ILs provided by different authors using the NRTL, eNRTL and UNIQUAC models.[18,61,62] For this reason,

no alternative models were tested with the present experimental data.

Application to ethanol purification

As mentioned above, the ternary phase diagrams here studied have a large biphasic region, and present different distribution coefficients from other ILs previously studied.[18] These observations raise the question on how these features can be used to build alternative ethanol purification schemes, with reduced energy requirements relative to the classical distillation approach. Since only LLE data of these systems were determined, and just at one temperature, the process alternatives here considered are focused on the potential use of these ILs as solvents for liquid–liquid extraction.

The medium ethanol concentration range is the region where higher liquid–liquid selectivities were observed towards this species. However, the use of this solution presupposes the existence of additional units for the initial ethanol concentration from the fermentation broth. Also, this is the region where distillation is more effective and strongly competes with alternative technologies, due to the larger relative volatility of ethanol. Furthermore, there are significant limitations to the direct use of liquid–liquid extraction in the high concentration region, since the biphasic envelope is much more limited in this concentration range. Hence, the use of liquid–liquid extraction is perhaps most effective in the low concentration regime.

The direct application of liquid–liquid extraction to the fermentation broth is restricted by the comparatively low selectivities (in the order of 5–6) observed in this region. This means that a large number of stages (coupled with large mass flow rates of IL) would be necessary to concentrate ethanol and to achieve a residue with a small concentration of this component. However, given the relatively large distribution coefficients registered here, a more favourable solution would be to use a single liquid–liquid extraction stage coupled to an extractive fermentation, where the IL is recycled continuously to the fermentator, as sketched in Fig. 10. This process configuration, while very distinct from the conventional batch fermentation typically used to achieve very high feed conversion, has already been investigated in detail with classical solvents.[63] One important advantage of this configuration is that it allows the recycling of the residue current back to the fermentator with a relatively high concentration of ethanol, where it can absorbs more ethanol before being reprocessed. The liquid–liquid extract has relatively poor water content, and therefore can be evaporated to originate a binary mixture with a significant ethanol concentration. If done under a slight vacuum, this evaporation can use residual heat that might be available in the process at low temperature levels, therefore having the potential to reduce the energy costs of the purification stage. Additional energy savings can also be contemplated by coupling various similar effects, operating at distinct pressures.

The proposed solution was tested with the ternary diagram containing the $[N(CN)_2]$-based IL for a 2 wt% of ethanol feed, using an equal mass of solvent. It is possible to conclude that the concentration of ethanol in the two phases is very similar, with an approximate total mass equi-distribution between the extract and residue currents. However, the mass concentration of water in the extract is much smaller than that in the residue. Due to this trend, complete evaporation of the extract leads to a mixture with approximately 65 wt% in ethanol. While smaller than the maximum ethanol extraction reported for this system (approximately 82%) this value is remarkable, since it is reachable with a single extraction step of a diluted solution, followed by evaporation of the extract. A further purification of this current towards anhydrous ethanol can be achieved through the application of a similar procedure (requiring in this case a much smaller solvent flow rate), in order to approach the maximum ethanol recovery possible by liquid–liquid extraction. For this purpose, the values presented in Table 1 become important to differentiate the behaviour between the various ILs studied.

As alternatives to the application of additional liquid–liquid extraction stages (given the previous considerations), available options include the use of conventional distillation up to the azeotrope followed by ethanol dehydration, or the use of pervaporation. In this last case, common specifications of anhydrous ethanol (99.5 wt%) are reachable for feeds with ethanol compositions in the range of 60–65 wt%, through the use of two consecutive pervaporation stages with hydrophilic membranes, and typical selectivities of $\alpha = 10$–12, using processing schemes similar to the one described by Roza and Maus.[64] This configuration would therefore allow the production of anhydrous ethanol from extractive fermentation, while completely avoiding the use of distillation in the purification phase. While potentially interesting, a comparison of the performance of this alternative with the more classical distillation-based approaches requires

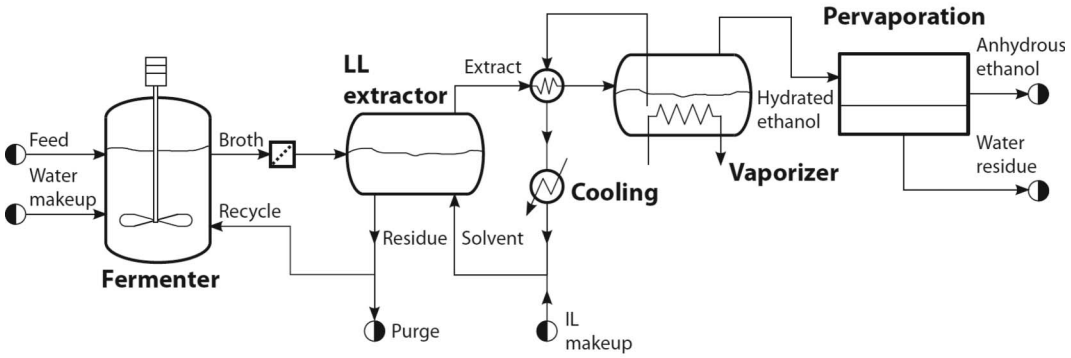

Fig. 10 Block diagram for ethanol purification based on liquid–liquid extraction and pervaporation.

a detailed evaluation of many aspects, not only related to the separation phase, but also relative to the reactor configuration and the interaction between these two processing phases, such as, the inhibition effects of the ILs and other metabolites present in the recycle stream, their path in the separation process and the consequent modifications in the simple scheme represented in Fig. 10 required to address them.

An additional paramount practical aspect of the use of ILs is their relative toxicity towards microorganisms. Unfortunately, toxicity data for phosphonium-based ILs are rather scarce in the literature. Yet, it was possible to retrieve the EC_{50} values for the enzymatic activity from the UFT/Merck ionic liquids biological effects database,[65] for the ILs studied in this work. Nevertheless, it should be remarked that enzyme assays may not be prime determinants for the microorganisms involved in fermentation processes. Most ILs affect cell membranes primarily and any enzyme effects would only be applicable for ILs that can cross such a membrane. The EC_{50} values are reported in Fig. 11 and are compared with various imidazolium-based counterparts, and also previously proposed for the water–ethanol separation process.[18] Values above 1000 μmol L^{-1} indicate a low inhibition potential. According to these results, the phosphonium-based ILs present a lower inhibition potential when compared with imidazolium-based solvents. With the exception of [TDTHP][$PF_3(C_2F_5)_3$], [TDTHP]Br and [TDTHP][CH_3SO_3], phosphonium ILs present low inhibition capacity. Therefore, in addition to the advantages previously discussed, the phosphonium-based ILs here proposed are also more favourable, concerning their toxicity, when compared with other ILs previously studied.

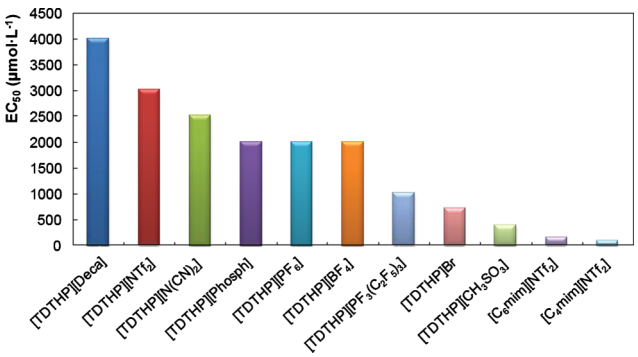

Fig. 11 EC_{50} values for the enzymatic activity in several ILs.[65]

Conclusions

Phosphonium-based ILs were evaluated in this work for potential use as solvents in the extraction of ethanol from fermentation broths. Ternary phase diagrams for seven distinct ILs, water and ethanol at 298 K were experimentally determined and presented. Predictions from the COSMO-RS model were evaluated against the experimental data and were mainly used to screen other ILs not experimentally studied. These simulations suggest that the [TDTHP][$C(CN)_3$] and [TDTHP][$B(CN)_4$] ILs are also potential alternatives for this purpose. A conceptual analysis of the alcohol recovery steps was carried out. As an alternative to classical distillation, a liquid–liquid extraction stage coupled to an extractive fermentation was proposed, where the IL is continuously recycled to the fermentator and the ethanol concentration is carried out by pervaporation, aiming at reducing the energy costs involved in the purification of ethanol.

Experimental section

Materials

The ternary systems IL + water + ethanol were determined for seven phosphonium-based ILs, namely, tetradecyltrihexylphosphonium chloride, [TDTHP]Cl (mass fraction purity ≈ 93–95%); tetradecyltrihexylphosphonium bromide, [TDTHP]Br (mass fraction purity ≈ 96–98%); tetradecyltrihexylphosphonium bis(trifluoromethylsulfonyl)imide, [TDTHP][NTf_2] (mass fraction purity > 98%); tetradecyltrihexylphosphonium bis(2,4,4-trimethylpentyl) phosphinate [TDTHP][Phosph] (mass fraction purity ≈ 93%); tetradecyltrihexylphosphonium decanoate, [TDTHP][Deca] (mass fraction purity ≈ 97%); tetradecyltrihexylphosphonium dicyanimide, [TDTHP][$N(CN)_2$] (mass fraction purity ≈ 97%) and tetradecyltrihexylphosphonium methanesulfonate [TDTHP][CH_3SO_3] (mass fraction purity ≈ 98–99%). The ILs molecular structures are shown in Fig. 1. All ILs were kindly provided by Cytec Industries Inc., and the mass fraction purities described correspond to the acquired commercial products. The chloride mass fraction content is < 10^{-3} for all samples.

Given the low purity of most ILs they were further purified by a repetitive washing procedure with ultrapure water and further dried under vacuum (10^{-5} Pa), at a moderate temperature (80 °C), and for at least 48 h. After this process, the purity of all ILs was evaluated by ^{31}P, ^{1}H, ^{13}C and ^{19}F NMR spectra, displaying purity mass fractions of > 99%. After the drying procedure, the water content in all samples was less than 5×10^{-4} in mass fraction as measured by Karl–Fischer titration. The ethanol used (EtOH, 2.6×10^{-4} of water in mass fraction) was > 99.8% pure from Riedel de Haën. The water used was double distilled, passed through a reverse osmosis system, and further treated with a Milli-Q plus 185 water purification apparatus.

Methods

To determine the tie-lines reported in this work, individual samples at various compositions of the three components (IL, water and EtOH) within the two phase region were prepared by weight, vigorously stirred, and allowed to reach equilibrium by phase separation for 12 h at 298 K. After this period and to ensure the complete separation of both phases, all samples were centrifuged at 3000 rpm for 20 min. A sample of ≈ 0.1 g was taken from both phases with a glass syringe and injected directly into a Metrohm 831 Karl–Fischer (KF) coulometer to determine the water content in each phase. In order to quantify the IL, a sample of ≈ (0.1 to 0.5) g of each phase was collected, weighed and further dried under moderated vacuum in a glass flask designed for the purpose to remove the water and EtOH. After this process, the IL content was determined by weight. The mass of EtOH in both phases was determined as the difference between the sample total mass and the mass of water and IL. For each sample and for each phase, at least three individual measurements were performed, with an average

uncertainty within 0.2 wt%. All the mass fraction quantifications were performed gravimetrically within ± 10^{-4} g.

The COSMO-RS calculations were performed at the BP/TZVP level (Turbomole,[66,67] DFT/COSMO calculation with the BP functional and TZVP[68] basis set using the optimized geometries at the same level of theory) with the parameter file BP_TZVP_C2.1_0110. The calculations were made for a multicomponent mixture where the cation and anion were treated as isolated species at equimolar conditions.

Acknowledgements

The authors acknowledge financial support provided by Fundação para a Ciência e a Tecnologia (Portugal) through the project PTDC/QUI/72903/2008, post-doctoral grant SFRH/BPD/41781/2007 of M. G. Freire and the Ph.D. grants SFRH/BD/70641/2010 and SFRH/BD/64338/2009 of Catarina M. S. S. Neves and J. F. Granjo, respectively.

References

1 E. Gnansounou and A. Dauriat, *Bioresour. Technol.*, 2010, **101**, 4980–4991.
2 H. J. Huang, S. Ramaswamy, U. W. Tschirner and B. V. Ramarao, *Sep. Purif. Technol.*, 2008, **62**, 1–21.
3 L. M. Vane, *Biofuels, Bioprod. Biorefin.*, 2008, **2**, 553–588.
4 M. Martín and I. E. Grossmann, in *ESCAPE20*, ed. S. Pierucci and G. B. Ferraris, Elsevier, Italy, 2010.
5 W. Arlt, M. Seiler, C. Jork and T. Sheneider, *DE Pat.*, 10 114 734, 2001.
6 M. Seiler, C. Jork, A. Kavarnou, W. Arlt and R. Hirsch, *AIChE J.*, 2004, **50**, 2439–2454.
7 N. Calvar, B. González, E. Gómez and Á. Domínguez, *J. Chem. Eng. Data*, 2008, **53**, 820–825.
8 W. Geng, L. Z. Zhang, D. S. Deng, Y. Ge and J. B. Ji, *J. Chem. Eng. Data*, 2010, **55**, 1679–1683.
9 A. V. Orchilles, P. J. Miguel, E. Vercher and A. Martinez-Andreu, *J. Chem. Eng. Data*, 2010, **55**, 1669–1674.
10 C. F. Poole and S. K. Poole, *J. Chromatogr., A*, 2010, **1217**, 2268–2286.
11 T. M. Boudreau and G. A. Hill, *Process Biochem.*, 2006, **41**, 980–983.
12 A. G. Fadeev and M. M. Meagher, *Chem. Commun.*, 2001, 295–296.
13 R. P. Swatloski, A. E. Visser, W. M. Reichert, G. A. Broker, L. M. Farina, J. D. Holbrey and R. D. Rogers, *Green Chem.*, 2002, **4**, 81–87.
14 V. Najdanovic-Visak, J. Esperanca, L. P. N. Rebelo, M. N. da Ponte, H. J. R. Guedes, K. R. Seddon and J. Szydlowski, *Phys. Chem. Chem. Phys.*, 2002, **4**, 1701–1703.
15 V. Najdanovic-Visak, A. Serbanovic, J. Esperanca, H. J. R. Guedes, L. P. N. Rebelo and M. N. da Ponte, *ChemPhysChem*, 2003, **4**, 520–522.
16 M. G. Freire, C. M. S. S. Neves, I. M. Marrucho, J. A. P. Coutinho and A. M. Fernandes, *J. Phys. Chem. A*, 2010, **114**, 3744–3749.
17 V. Najdanovic-Visak, L. P. N. Rebelo and M. N. da Ponte, *Green Chem.*, 2005, **7**, 443–450.
18 A. Chapeaux, L. D. Simoni, T. S. Ronan, M. A. Stadtherr and J. F. Brennecke, *Green Chem.*, 2008, **10**, 1301–1306.
19 C. J. Bradaric, A. Downard, C. Kennedy, A. J. Robertson and Y. H. Zhou, *Green Chem.*, 2003, **5**, 143–152.
20 N. V. Plechkova and K. R. Seddon, *Chem. Soc. Rev.*, 2008, **37**, 123–150.
21 U. Domańska and L. M. Casás, *J. Phys. Chem. B*, 2007, **111**, 4109–4115.
22 U. Domańska and K. Paduszyński, *J. Phys. Chem. B*, 2008, **112**, 11054–11059.
23 U. Domańska and K. Paduszyński, *Fluid Phase Equilib.*, 2009, **278**, 90–96.
24 U. Domańska and K. Paduszyński, *J. Chem. Thermodyn.*, 2010, **42**, 707–711.
25 L. I. N. Tomé, R. L. Gardas, P. J. Carvalho, M. J. Pastoriza-Gallego, M. M. Piñeiro and J. A. P. Coutinho, *J. Chem. Eng. Data*, 2011, DOI: 10.1021/je101232g.
26 C. M. S. S. Neves, P. J. Carvalho, M. G. Freire and J. A. P. Coutinho, *J. Chem. Thermodyn.*, 2011, **43**, 948–957.
27 M. G. Freire, P. J. Carvalho, R. L. Gardas, L. M. N. B. F. Santos, I. M. Marrucho and J. A. P. Coutinho, *J. Chem. Eng. Data*, 2008, **53**, 2378–2382.
28 P. J. Carvalho, V. H. Álvarez, I. M. Marrucho, M. Aznar and J. A. P. Coutinho, *J. Supercrit. Fluids*, 2010, **52**, 258–265.
29 P. J. Carvalho and J. A. P. Coutinho, *J. Phys. Chem. Lett.*, 2010, **1**, 774–780.
30 S. P. M. Ventura, J. Pauly, J. L. Daridon, J. A. Lopes da Silva, I. M. Marrucho, A. M. A. Dias and J. A. P. Coutinho, *J. Chem. Thermodyn.*, 2008, **40**, 1187–1192.
31 F. S. Oliveira, M. G. Freire, M. J. Pratas, J. Pauly, J. L. Daridon, I. M. Marrucho and J. A. P. Coutinho, *J. Chem. Eng. Data*, 2009, **55**, 662–665.
32 C. L. S. Louros, A. F. M. Cláudio, C. M. S. S. Neves, M. G. Freire, I. M. Marrucho, J. Pauly and J. A. P. Coutinho, *Int. J. Mol. Sci.*, 2010, **11**, 1777–1791.
33 D. Othmer and P. Tobias, *Ind. Eng. Chem.*, 1942, **34**, 693–696.
34 J. D. Seader and E. J. Henley, in *Separation Process Principles*, John Wiley & Sons, New York, edn, 1998.
35 X. S. Hu, J. Yu and H. Z. Liu, *J. Chem. Eng. Data*, 2006, **51**, 691–695.
36 F. Eckert and A. Klamt, *AIChE J.*, 2002, **48**, 369–385.
37 A. Klamt, *J. Phys. Chem.*, 1995, **99**, 2224–2235.
38 A. Klamt, in *COSMO-RS from Quantum Chemistry to Fluid Phase Thermodynamics and Drug Design*, Elsevier, Amsterdam, 1st edn, 2005.
39 A. Klamt and F. Eckert, *Fluid Phase Equilib.*, 2000, **172**, 43–72.
40 A. Klamt and G. Schuurmann, *J. Chem. Soc., Perkin Trans. 2*, 1993, 799–805.
41 U. Domanska, A. Pobudkowska and F. Eckert, *J. Chem. Thermodyn.*, 2006, **38**, 685–695.
42 U. Domańska, A. Pobudkowska and F. Eckert, *Green Chem.*, 2006, **8**, 268–276.
43 M. G. Freire, P. J. Carvalho, R. L. Gardas, I. M. Marrucho, L. M. N. B. F. Santos and J. A. P. Coutinho, *J. Phys. Chem. B*, 2008, **112**, 1604–1610.
44 M. G. Freire, C. M. S. S. Neves, P. J. Carvalho, R. L. Gardas, A. M. Fernandes, I. M. Marrucho, L. M. N. B. F. Santos and J. A. P. Coutinho, *J. Phys. Chem. B*, 2007, **111**, 13082–13089.
45 M. G. Freire, L. M. N. B. F. Santos, I. M. Marrucho and J. A. P. Coutinho, *Fluid Phase Equilib.*, 2007, **255**, 167–178.
46 M. G. Freire, S. P. M. Ventura, L. M. N. B. F. Santos, I. M. Marrucho and J. A. P. Coutinho, *Fluid Phase Equilib.*, 2008, **268**, 74–84.
47 K. Marsh, A. Deev, A. Wu, E. Tran and A. Klamt, *Korean J. Chem. Eng.*, 2002, **19**, 357–362.
48 K. Sahandzhieva, D. Tuma, S. Breyer, Á. Pérez-Salado Kamps and G. Maurer, *J. Chem. Eng. Data*, 2006, **51**, 1516–1525.
49 C. T. Wu, K. N. Marsh, A. V. Deev and J. A. Boxall, *J. Chem. Eng. Data*, 2003, **48**, 486–491.
50 T. Banerjee, K. K. Verma and A. Khanna, *AIChE J.*, 2008, **54**, 1874–1885.
51 A. A. P. Kumar and T. Banerjee, *Fluid Phase Equilib.*, 2009, **278**, 1–8.
52 Z. G. Lei, W. Arlt and P. Wasserscheid, *Fluid Phase Equilib.*, 2007, **260**, 29–35.
53 M. G. Freire, P. J. Carvalho, L. M. N. B. F. Santos, L. R. Gomes, I. M. Marrucho and J. A. P. Coutinho, *J. Chem. Thermodyn.*, 2010, **42**, 213–219.
54 A. R. Ferreira, M. G. Freire, J. C. Ribeiro, F. M. Lopes, J. G. Crespo and J. A. P. Coutinho, *Ind. Eng. Chem. Res.*, 2011, DOI: 10.1021/ie102471b.
55 H. Renon and J. M. Prausnitz, *AIChE J.*, 1968, **14**, 135–144.
56 L. D. Simoni, J. F. Brennecke and M. A. Stadtherr, *Ind. Eng. Chem. Res.*, 2009, **48**, 7246–7256.
57 L. D. Simoni, A. Chapeaux, J. F. Brennecke and M. A. Stadtherr, *Ind. Eng. Chem. Res.*, 2009, **48**, 7257–7265.
58 L. D. Simoni, Y. Lin, J. F. Brennecke and M. A. Stadtherr, *Fluid Phase Equilib.*, 2007, **255**, 138–146.
59 L. D. Simoni, Y. Lin, J. F. Brennecke and M. A. Stadtherr, *Ind. Eng. Chem. Res.*, 2007, **47**, 256–272.
60 J. M. Sørensen, T. Magnussen, P. Rasmussen and A. Fredenslund, *Fluid Phase Equilib.*, 1979, **3**, 47–82.

61 Y. Song and C.-C. Chen, *Ind. Eng. Chem. Res.*, 2009, **48**, 7788–7797.
62 L. D. Simoni, A. Chapeaux, J. F. Brennecke and M. A. Stadtherr, *Comput. Chem. Eng.*, 2010, **34**, 1406–1412.
63 M. Matsumura and H. Märkl, *Appl. Microbiol. Biotechnol.*, 1984, **20**, 371–377.
64 M. Roza and E. Maus, in *Distillation & Absorption 2006*, ed. E. Sørenson, IChemE, Rugby, 2006.
65 http://www.il-eco.uft.uni-bremen.de, accessed December 3rd, 2010.
66 R. Ahlrichs, M. Bär, M. Häser, H. Horn and C. Kölmel, *Chem. Phys. Lett.*, 1989, **162**, 165–169.
67 A. Schäfer, A. Klamt, D. Sattel, J. C. W. Lohrenz and F. Eckert, *Phys. Chem. Chem. Phys.*, 2000, **2**, 2187–2193.
68 A. Schäfer, C. Huber and R. Ahlrichs, *J. Chem. Phys.*, 1994, **100**, 5829–5835.

